Original Article

Check for updates

Available online at
www.heca-analitika.com/malacca_pharmaceutics

Malacca Pharmaceutics

Vol. 2, No. 1, 2024

Exploring the Medicinal Potential of *Blumea balsamifera*: Insights from Molecular Docking and Molecular Dynamics Simulations Analyses

Nur Balqis Maulydia [1], Khairan Khairan [2], Trina Ekawati Tallei [3], Salaswati Salaswati [4], Annisa Musdalifah [4], Fiki Farah Nabila [2] and Rinaldi Idroes [2,4,*]

[1] Graduate School of Mathematics and Applied Sciences, Universitas Syiah Kuala, Banda Aceh 23111, Indonesia; maulydiabalqis@gmail.com (N.B.M)
[2] Department of Pharmacy, Faculty Mathematics and Natural Sciences, Universitas Syiah Kuala, Banda Aceh 23111, Indonesia; khairankhairan@usk.ac.id (K.K.); fikifarahnabila@gmail.com (F.F.N); rinaldi.idroes@usk.ac.id (R.I)
[3] Department of Biology, Faculty Mathematics and Natural Sciences, Universitas Sam Ratulangi, Manado 95115, Indonesia; trina_tallei@unsrat.ac.id (T.E.T)
[4] Department of Chemistry, Faculty Mathematics and Natural Sciences, Universitas Syiah Kuala, Banda Aceh 23111, Indonesia; salaswati7@gmail.com (S.S); annisamusdalifah171931@gmail.com (A.M)

* Correspondence: rinaldi.idroes@usk.ac.id

Article History

Received 24 January 2024
Revised 16 March 2024
Accepted 25 March 2024
Available Online 31 March 2024

Keywords:
Ie-Jue
GC-MS
Stigmasterol
Geothermal area

Abstract

Blumea balsamifera from the Ie-Jue geothermal area in Aceh Province, Indonesia, has been reported to have a variety of secondary metabolites. However, there is limited information about the activity of these chemical metabolites from *B. balsamifera*. The aim of this study is to evaluate the therapeutic potential of these compounds using molecular docking and molecular dynamics simulations. Six selective compounds were thoroughly evaluated using molecular docking techniques for their inhibitory effects on both Coronavirus protease and human interleukin receptors. Additionally, druglikeness assessments based on the Lipinski rule of five were performed to evaluate these six ligands. Our results show that stigmasterol, a key component of *B. balsamifera*, has demonstrated low binding free energy values across four receptors. Furthermore, molecular dynamics simulations confirmed the stability of the top ligand-receptor complex, particularly stigmasterol-1IRA, based on five parameters, indicating its stability as an inhibitor. This research highlights the potential of stigmasterol as a therapeutic agent derived from medicinal plants of *B. balsamifera* and underscores the value of our molecular approach in identifying opportunities for pharmaceutical development.

1. Introduction

Nature provides an abundance of plants from which to conduct research on the type of active compound. The biosynthesis processes of secondary metabolites are heavily influenced by their geographic location and habitat [1, 2]. One of the areas that has characteristic environmental conditions is the earth's hot area or geothermal manifestation [3, 4]. In response to earth heat, some plants in this earth heat region produce secondary metabolites in higher and more varied amounts.

Previous research has shown that there is a difference in secondary metabolite content between geothermal and non-geothermal plants, with the extract of the leaf (*Vitex pinnata* L) from the positive geothermal area containing a flavonoid compound, whereas the extracts of the leaf

from the non-geothermal region do not [5]. One of the areas in Sumatra Island, Indonesia, that has the potential for earth's heat energy is Aceh Province, where one of the geothermal areas is the Jue geothermal area in Seulimeum district, Aceh Besar [6, 7].

One application for secondary metabolite compounds in drug development is the management and treatment of virally induced illnesses [8]. A class of viruses known as coronaviruses typically targets the respiratory system, resulting in acute respiratory tract infections that have been linked to a pandemic of severe acute respiratory syndrome-coronavirus 2 (SARS-CoV-2) for several years [9].

Currently, the discovery and development of drugs against the SARS-CoV-2 protein using the computational approach known as in silico is constantly evolving, particularly in the treatment of SARS-CoV-2 infections. One approach that could be used is molecular docking, which allows researchers to use three-dimensional structure information for biological targets to see binding energies, molecule interactions, and changes in conformation structure for examining metabolite compounds or ligands [10].

Previous in silico research on the development of drugs to treat COVID-19 patients found that secondary metabolite compounds such as amentoflavone, 7-O-galloylquercetin, kaempferitrin, and gallagic acid, a secondary flavonoid metabolite, can inhibit some proteins involved in the SARS-CoV-2 life cycle such as protease (M^{pro} and PL^{pro}), RNA-dependent RNA polymerase (RdRp), and Spike protein with stable binding conformation [11]. According to other research, compounds classified as secondary metabolites, like andrographolide, have been shown to be effective in inhibiting interleukin [12]. Based on the findings of these studies, secondary metabolite compounds can inhibit the proteins involved in the SARS-CoV-2 life cycle as well as the protein that causes cytokine storm syndrome.

Our previous study revealed that *Blumea balsamifera*, a medicinal plant in the Ie-Jue geothermal area, contains a wide range of secondary metabolites [13]. However, limited research has been conducted on this plant, particularly using molecular docking. As a result, the purpose of this study is to determine the therapeutic potential of active plant compounds from the Ie-Jue areas, namely *B. balsamifera*, against SARS-CoV-2 protease (M^{pro} and PL^{pro}) and pro-inflammatory cytokines (IL-1 and IL-6) using molecular docking and molecular dynamics simulations. This study not only identified the active compound in *B. balsamifera* but also demonstrated the plant's potential for drug discovery.

2. Materials and Methods

2.1. Druglikeness Assessment

Six molecules that were identified as metabolites of *B. balsamifera* in our earlier research were used as ligands based on relative area, namely proximadiol (41.76%), phytol (6.84%), endo-borneol (0.77%), β-acorenol (0.65%), stigmasterol (4.46%), and hexadecenoic acid, methyl ester (8.54%) [13]. The druglikeness was examined using the Lipinski rule of five (Ro5) in SwissADME based on their SMILES structure (Table 1) [14]. Lipinski rules consist of four parameters, namely molecular weight less than 500 g/mol, donor hydrogen (<5), acceptor hydrogen (<10), and Moriguchi Log P (MLogP) rule ≤ 4.15 [15].

2.2. Ligand Preparations of Molecular Docking

Molecular docking consists of two preparations: ligand preparations and receptor preparations. In ligand preparations, the 3D chemical structure of six compounds was retrieved from the PubChem database to download the SDF file [16]. Next, minimization of energy was conducted using PyRx [17]. The list of ligands is displayed in Table 1.

2.3. Receptors Preparations of Molecular Docking

Four receptors used in this study were obtained from the protein data bank [18]. There are the main protease (M^{pro}) and papain-like protease (PL^{pro}) of SARS-CoV-2, and interleukin-1 (IL-1) and interleukin-6 (IL-6) of *Homo sapiens* (Figure 1). The selection of receptors based on the activity of these receptors is part of the cytokine storm syndrome in clinical studies [19]. As shown in Figure 1, receptor preparations include the removal of native ligands and water molecules using BIOVIA Discovery Visualizer Software [20]. The molecular docking process has been examined using Autodock Vina [21] with selective grid box and specific docking. Molecular docking results are visualized using PoseView (Universität Hamburg, Germany) and BIOVIA Discovery Visualizer Software [20, 22]. The visualization includes hydrogen bonds and hydrophobic interactions between complex ligands and receptors.

2.4. Molecular Dynamics simulations

Molecular dynamics simulation was conducted using Visual Molecular Dynamics (VMD) - Nanoscale Molecular Dynamics (NAMD) [23, 24]. The Charmm-gui website was used to build the receptor molecular topology and configuration files [25]. The simulated system was neutralized by the addition of 0.15 M KCl. Next, the water molecules box TIP3PBOX was immersed in the neutralized system. Before the production phase, each system was equilibrated with NVT (constant number of

Table 1. Metabolite compounds of *B. balsamifera.*

No	Compounds name	SMILES	PubChem CID
1	Proximadiol	CC12CCCC(C1CC(CC2)C(C)(C)O)(C)O	165258
2	Phytol	CC(C)CCCC(C)CCCC(C)CCCC(=CCO)C	5280435
3	Endo-borneol	CC1(C2CCC1(C(C2)O)C)C	6552009
4	β-Acorenol	CC1CCC(C12CCC(=C)CC2)C(C)(C)O	6430766
5	Stigmasterol	CCC(C=CC(C)C1CCC2C1(CCC3C2CC=C4C3(CCC(C4)O)C)C)C(C)C	5280794
6	Hexadecanoic acid, methyl ester	CCCCCCCCCCCCCCCC(=O)OC	8181

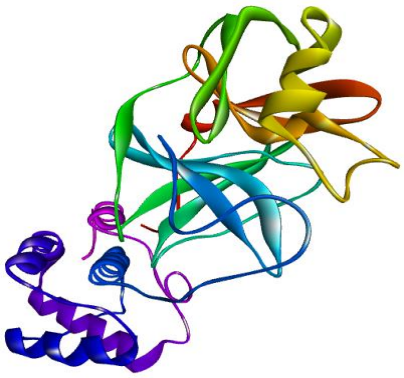

(a) Main protease (PDB ID: 6LU7)

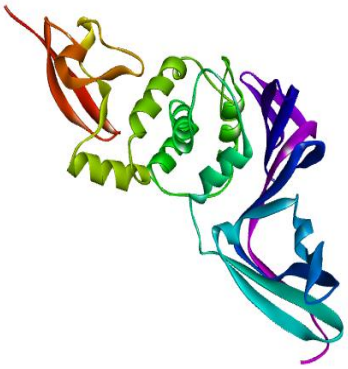

(b) Papain-like protease (PDB ID: 6WX4)

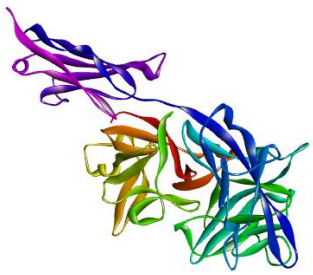

(c) Interleukin-1 (PDB ID: 1IRA)

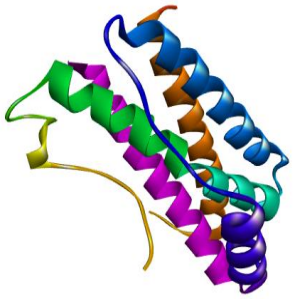

(d) Interleukin-6 (PDB ID: 1ALU)

Figure 1. The four receptors.

particles, volume, and temperature) and NPT (constant number of particles, pressure, and temperature) to ensure a uniform distribution of ions and solvent around the protein–ligand complex.

3. Results and Discussion

The similarity of a chemical compound to a drug (druglikeness) can be evaluated using a variety of parameters. One of the most widely used parameters is Lipinski's Rule of Five (Ro5) [26]. According to Lipinski's rule, an orally active drug should not have more than one violation of the established criteria. Therefore, it is examined whether the six docking compounds meet Ro5. Based on Table 2, it can be observed that all docking compounds have a molecular weight of less than 500 g/mol, donor-binding-H (<5), binding-H-acceptor (<10), but there are some compounds that violate the MLogP rule ≤ 4.15 but the violation still meet to Ro5 [15].

Molecular docking aims to determine how the test ligand and receptor interact in a biological process [27]. This docking study provides important information about the binding mechanisms and bond affinity between the ligand and the target protein. The first step in the docking process involves predicting the orientation, shape, and location of the ligand within the protein binding site. The bonding quality is then evaluated using the assessment scoring function. The Gibbs affinity or binding free energy value (ΔG) is used as the scoring function; the stronger the complex bond between the ligands and the receptors, the smaller or more negative the Gibbs affinities/free energies (ΔG) that are generated during the ligand and receptor interaction [28]. In this work, four

Table 2. Druglikeness evaluation using Ro5.

No	Compounds name	Lipinski Rule of Five					Meet Ro5
		MW (<500) (g/mol)	(LogP) ≤ 4,15	Donor H-bond (<5)	Acceptor H-bond (<10)	Violations	
1	Proximadiol	240.38	2.88	2	2	0	Yes
2	Phytol	296.53	5.25	1	1	1	Yes
3	Endo-borneol	154.25	2.45	1	1	0	Yes
4	β-Acorenol	222.37	3.67	1	1	0	Yes
5	Stigmasterol	412.69	6.62	1	1	1	Yes
6	Hexadecanoic acid, methyl ester	270.45	4.44	0	2	1	Yes

Descriptions: MW= Molecular weight

Table 3. Molecular docking results.

No	Compounds name	6LU7	6WX4	1IRA	1ALU
		Binding free energy (kcal/mol)			
-	Positive control	-8.4	-7	-7.1	-6.9
1	Stigmasterol	-7.8	-7.5	-8.5	-7.3
2	β-acorenol	-6	-5.8	-6.7	-6.6
3	Proximadiol	-6.2	-5.9	-6.7	-6.2
4	Endo-borneol	-5.7	-4.9	-6.8	-5.6
5	Phytol	-5.3	-5.3	-6.5	-4.6
6	Hexadecanoic acid, methyl ester	-4.3	-4.6	-4.9	-4.3

receptors were targeted by molecular docking: two of the receptors for the SARS-CoV-2 virus proteins are papain-like proteases (PL^{pro}) and main protease (M^{pro}), while two of the receptors for inflammatory cytokines are Interleukin-1 (IL-1) and Interleukine-6 (IL-6). Nefinavir, a protease inhibitor, is the positive control used for M^{pro} and PL^{pro} [10]. The results are shown in Table 3.

Based on Table 3, the binding free energy of several compounds from the ethanolic extract *B. balsamifera* from Ie-Jue has varying values. Stigmasterol demonstrated the lowest values, indicating a higher affinity for its interactions. Stigmasterol, a phytosterol that is a member of the tetracyclic triterpene class of steroids—also referred to as stigmasterin—has a structure resembling that of cholesterol. The bioactivities of stigmasterol, including its anti-inflammatory, immunomodulatory, neuroprotective, antibacterial, antifungal, antioxidant, antidiabetic, and antiviral properties, have been demonstrated in a number of studies [29]. The results of Kamaz et al. [30] also showed that the molecular docking of stigmasterol showed a strong ability to interact with the spike protein of SARS-CoV-2.

Molecular docking of stigmasterol with M^{pro} and PL^{pro} showed two hydrogen bonds between Glu: 228 and Ala: 230. Hydrophobic interactions were also found around the ligands, namely Val: 164, Phe: 161, Lys: 179, Thr: 291, Met: 281, Leu: 181 and Gly: 159 in M^{pro} (Figure 2a) with a binding affinity of -7.8 kcal/mol approaching its positive control affinities, and Met: 281 in PL^{pro} (Figure 2b) with binding affinity values of -7.5 kcal/mol lower than the positive binding value of the control. Molecular docking between stigmasterol and IL-1 has a bonding affinity of -8.5 kcal/mol lower than the positive control bonding. The interactions that occurred were hydrogen bond Gln: 125 and hydrophobic interactions: Tyr: 119, Leu: 120, Tyr: 119, and Leu: 55 (Figure 2c). Molecular docking of stigmasterol with IL-6 showed the existence of hydrogen bond in Asn: 257 and hydrophobic interactions: Glu: 324, and Ala: 250 (Figure 2d) with binding affinity values of -7.3 kcal/mol lower than their positive control affinities. The binding affinity of M^{pro} with the positive control, nelfinavir, is -8.4 kcal/mol. Interactions include hydrogen bonding, π-σ interactions, alkyl interactions, amide-π stacking, π-alkyl interactions, and Van der Waals interactions (Figure 3a). Molecular docking against PL^{pro} with nelfinavir showed the occurrence of hydrogen bonding, alkyl interaction, π-alkyl, and van der Waals interaction (Figure 3b) with a binding affinity of -7 kcal/mol.

The most abundant compound, proximadiol, has a value of -6.2 kcal/mol in M^{pro} and -5.9 kcal/mol in PL^{pro} as well as -6.7 kcal/mol to IL-1 and -6.2 kcal/mol to IL-6. Proximadiol has the potential to have anti-inflammatory activity based on the PASS prediction, with a Pa prediction of 0.776 [13]. It is known that this substance has valuable potential for anti-inflammatory action when combined with interleukin inhibitory activity. Proximadiol also found in *Cymbopogon proximus* [31]. Other compounds, such as β-acorenol, that were also identified in V. pinnata from the Ie-Seu'um geothermal area [32], demonstrated a greater chance of interaction with -6 kcal/mol to M^{pro} and -5.8 to PL^{pro}.

In this work, we conducted molecular dynamics simulations using stigmasterol-1IRA, one of the top

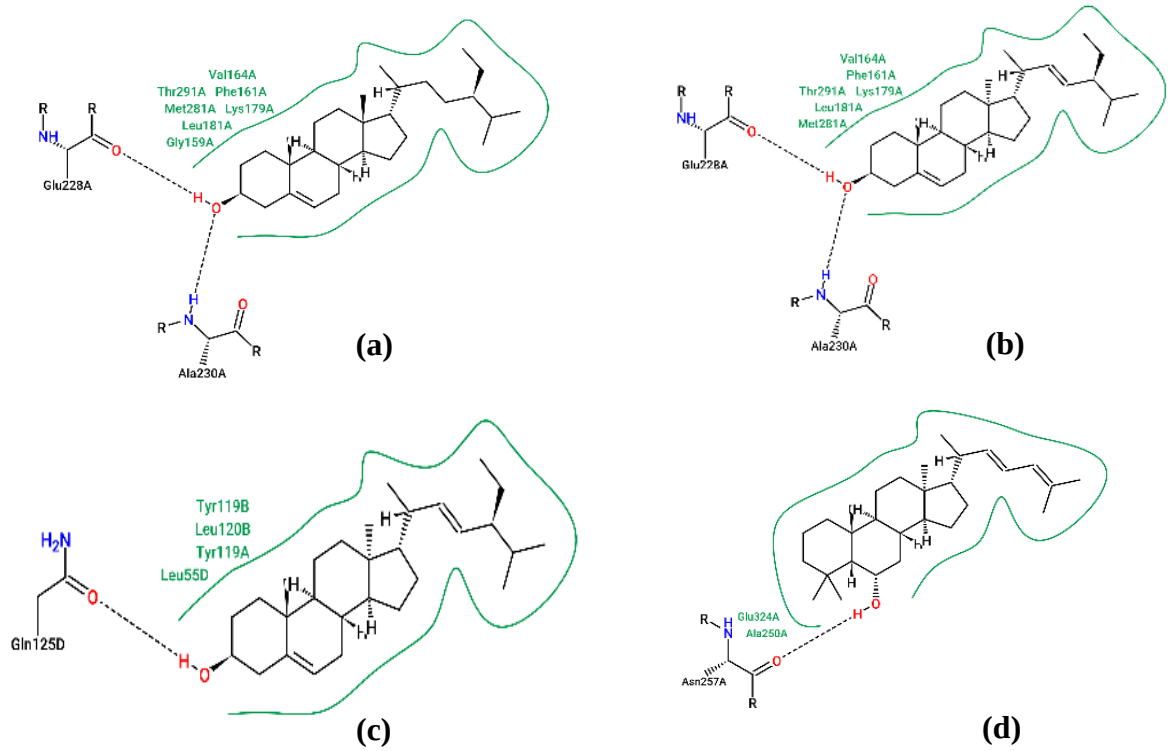

Figure 2. Two-dimensional interactions of stigmasterol with four receptors. (a) M^{pro}, (b) PL^{pro}, (c) IL-1, and (d) IL-6.

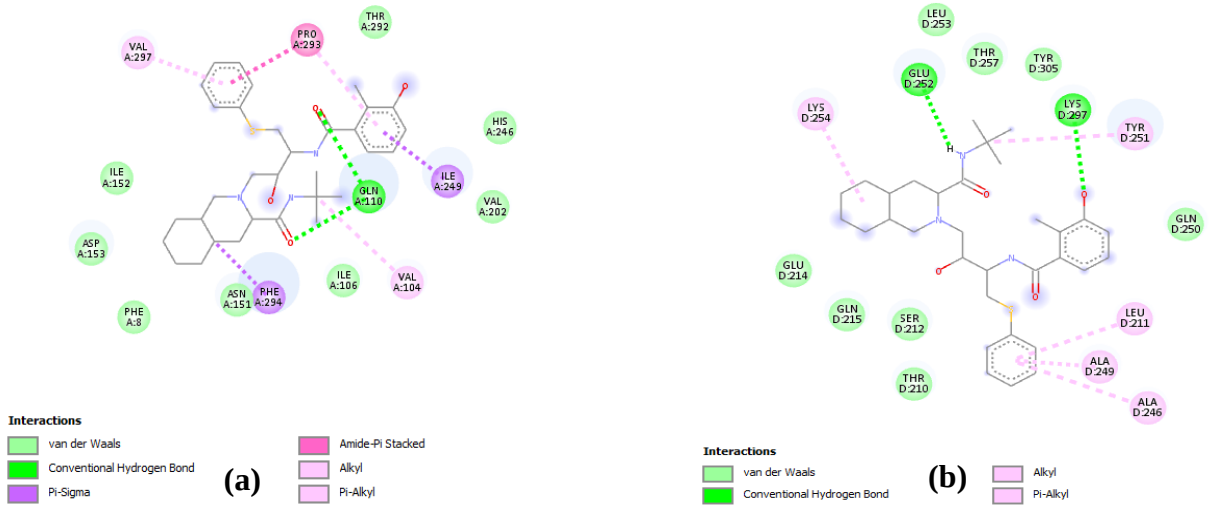

Figure 3. Two-dimensional interactions of nelvinafir in M^{pro} and PL^{pro}.

compound-target dockings. The molecular dynamics studies on stigmasterol have revealed interesting findings. Five parameters were assessed in MDs: root mean square deviation (RMSD), root mean square fluctuation (RMSF), the radius of gyration (RG), solvent accessible surface area (SASA), and hydrogen bond (Figure 4). The RMSD curve illustrates protein positional deviations. Figure 4a shows that RMSD curves stabilized after 0.2 to 1 ns. This means that the ligand is completely bonded to the receptor. The protein's fluctuations in amino acid residues are depicted by the RMSF curve. The variation in 50 was displayed in Figure 4b by the RMSF values of residue numbers 50–150 in the 1IRA. Next, the tightness of the protein's overall structure is indicated by the rotation curve's radius (radius of gyration in nm). The rotation radii of the stigmasterol–1IRA complexes were stable, as shown in Figure 4c. As a complement to the parameters, SASA displayed a similar curve with radius of gyration. As seen in Figure 4d. the elevation of surface area varies with time, just like radii. This means that radii and surface area influence the rotation of complex ligand receptors. The last hydrogen bond in Figure 4e demonstrated an increase in the number of hydrogen bonds over time. This is related to the stability of the

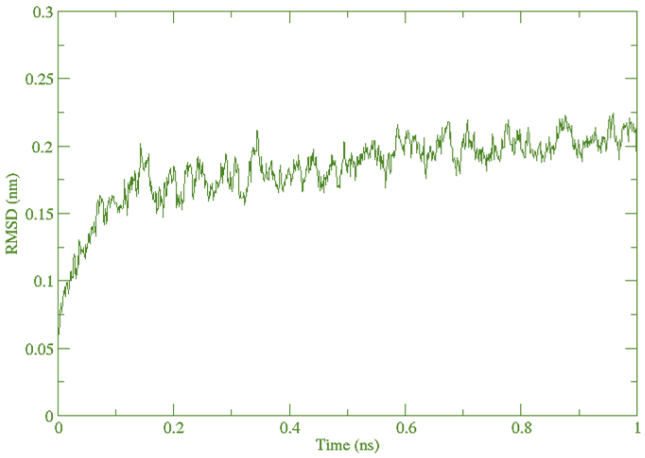

(a) RMSD

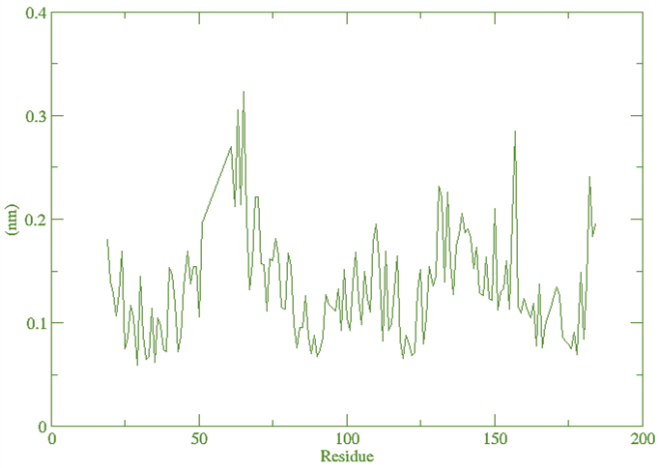

(b) RMSF

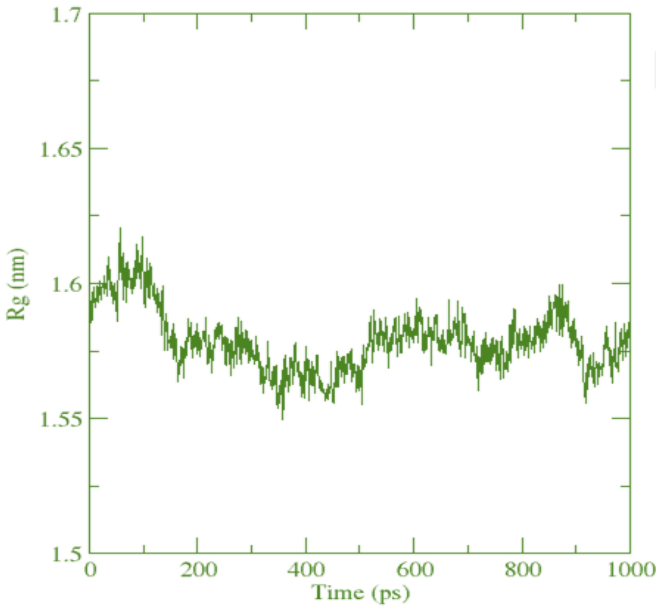

(c) radius of gyration

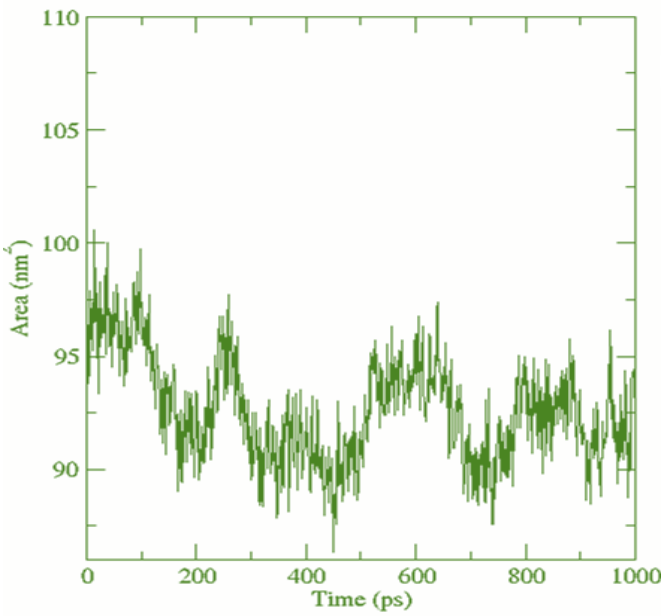

(d) SASA

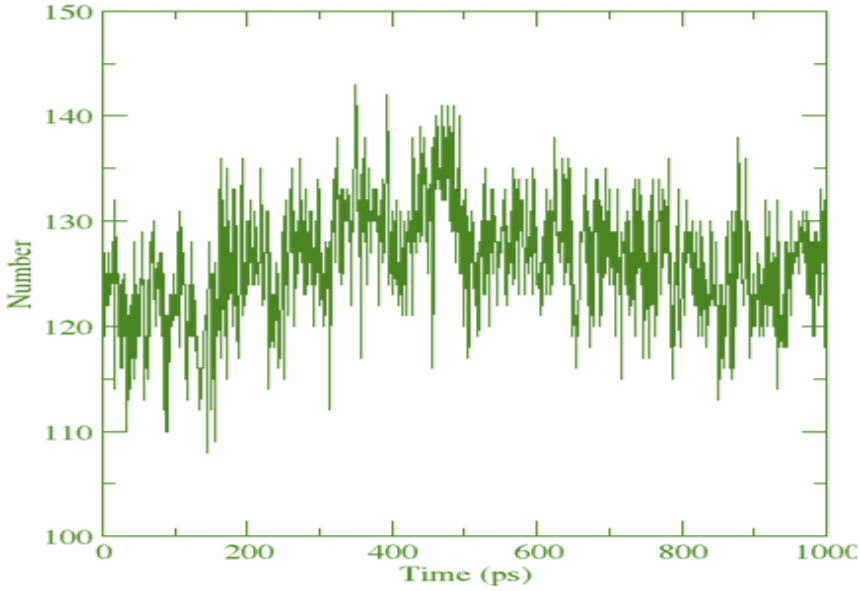

(e) hydrogen bond

Figure 4. Parameters of molecular dynamics simulations.

complex as long as the MDs are running. Overall, the parameter demonstrated the stability of complex ligand-receptor interactions.

4. Conclusions

In conclusion, our study highlights the medicinal potential of *B. balsamifera*, particularly through the promising compound stigmasterol, as revealed by molecular docking and dynamics analyses. The consistently low binding free energy values across multiple receptors suggest stigmasterol's efficacy as a therapeutic agent against both Coronavirus protease and human interleukin receptors. Additionally, the stability of the stigmasterol-1IRA ligand-receptor complex underscores its potential for further pharmaceutical development. These findings underscore the significance of natural products like those found in *B. balsamifera* in drug discovery and development efforts. Further research and clinical studies are warranted to fully elucidate the therapeutic benefits of these compounds and their potential contribution to combating viral infections and inflammatory disorders.

Author Contributions: Conceptualization, N.B.M., K.K. and R.I; methodology, N.B.M., and S.S.; software, N.B.M., S.S., A.M. and F.F.N; validation, K.K., T.E.T. and R.I.; formal analysis, T.E.T.; investigation, N.B.M.; resources, K.K. and R.I; data curation, T.E.T.; writing—original draft preparation, N.B.M.; writing—review and editing, N.B.M. and S.S.; visualization, N.B.M.; supervision, T.E.T. and R.I; project administration, K.K. All authors have read and agreed to the published version of the manuscript.

Funding: This research was funded by Kementerian Pendidikan, Kebudayaan, Riset dan Teknologi Nasional through the "Program Magister menuju Doktor untuk Sarjana Unggul" scheme, grant number: 585/UN11.2.1/PT.01.03/DRPM/2023.

Ethical Clearance: Not applicable.

Informed Consent Statement: Not applicable.

Data Availability Statement: Further inquiries data can be directed to the corresponding author.

Conflicts of Interest: All the authors declare that there are no conflicts of interest.

References

1. Imelda, E., Khairan, K., Lubis, R. R., Karma, T., and Idroes, R. (2024). Impact of Environmental and Geographical Position on the Chemometric Classification of Ethanol Extracts from Isotoma longiflora Leaves, *Global Journal of Environmental Science and Management*, Vol. 10, No. 1, 155–168. doi:10.22034/gjesm.2024.01.11.
2. Maulydia, N. B., Idroes, R., Khairan, K., Tallei, T. E., and Mohd Fauzi, F. (2024). Ecotoxicological Insight of Phytochemicals, Toxicological Informatics, and Heavy Metal Concentration in Tridax procumbens L. in Geothermal Areas, *Global Journal of Environmental Science and Management*, Vol. 10, No. 1, 369–384. doi:10.22034/gjesm.2024.01.23.
3. Idroes, R., Khairan, K., and Fakri, F. (2017). *Screening of Potential Plant Activities as Antimicrobial Materials in the Ie Jue Area (Upflow Geothermal Zone) Aceh Besar*, Syiah Kuala University Press, Banda Aceh.
4. Fakri, F., Harahap, S. P., Muhni, A., Khairan, K., Hewindati, Y. T., and Idroes, G. M. (2023). Antimicrobial Properties of Medicinal Plants in the Lower Area of Ie Seu-um Geothermal Outflow, Indonesia, *Malacca Pharmaceutics*, Vol. 1, No. 2, 55–61. doi:10.60084/mp.v1i2.44.
5. Nuraskin, C., Marlina, Idroes, R., Soraya, C., and Djufri. (2020). Identification of Secondary Metabolite of Laban Leaf Extract (Vitex pinnata L) from Geothermal Areas and Non-Geothermal of Agam Mountains in Aceh Besar, Aceh Province, Indonesia, *Rasayan Journal of Chemistry*, Vol. 13, No. 1, 18–23. doi:10.31788/RJC.2020.1315434.
6. Idroes, R., Yusuf, M., Saiful, S., Alatas, M., Subhan, S., Lala, A., Muslem, M., Suhendra, R., Idroes, G. M., Marwan, M., and Mahlia, T. M. I. (2019). Geochemistry Exploration and Geothermometry Application in the North Zone of Seulawah Agam, Aceh Besar District, Indonesia, *Energies*, Vol. 12, No. 23, 4442. doi:10.3390/en12234442.
7. Aprianto, A., Maulana, A., Noviandy, T. R., Lala, A., Yusuf, M., Marwan, M., Afidh, R. P. F., Irvanizam, I., Nizamuddin, N., and Idroes, G. M. (2023). Exploring Geothermal Manifestations in Ie Jue , Indonesia : Enhancing Safety with Unmanned Aerial Vehicle, *Leuser Journal of Environmental Studies*, Vol. 1, No. 2, 47–54. doi:10.60084/ljes.v1i2.75.
8. Tallei, T. E., Fatimawali, Yelnetty, A., Idroes, R., Kusumawaty, D., Emran, T. Bin, Yesiloglu, T. Z., Sippl, W., Mahmud, S., Alqahtani, T., Alqahtani, A. M., Asiri, S., Rahmatullah, M., Jahan, R., Khan, M. A., and Celik, I. (2021). An Analysis Based on Molecular Docking and Molecular Dynamics Simulation Study of Bromelain as Anti-SARS-CoV-2 Variants, *Frontiers in Pharmacology*, Vol. 12, No. August, 1–18. doi:10.3389/fphar.2021.717757.
9. Tallei, T. E., Tumilaar, S. G., Niode, N. J., Fatimawali, Kepel, B. J., Idroes, R., Effendi, Y., Sakib, S. A., and Emran, T. Bin. (2020). Potential of Plant Bioactive Compounds as SARS-CoV-2 Main Protease (Mpro) and Spike (S) Glycoprotein Inhibitors: A Molecular Docking Study, *Scientifica*, Vol. 2020, 1–18. doi:10.1155/2020/6307457.
10. Maulydia, N. B., Tallei, T. E., Ginting, B., Idroes, R., Illian, D. N., and Faradilla, M. (2022). Analysis of Flavonoid Compounds of Orange (Citrus sp.) Peel As Anti-Main Protease of SARS-CoV-2: A Molecular Docking Study, *IOP Conference Series: Earth and Environmental Science*, Vol. 951, No. 1, 012078. doi:10.1088/1755-1315/951/1/012078.
11. Jorge, A., Lopes, O., Calado, G. P., Nascimento, Y., Alves, S., Ara, D., França, L. M., Marcus, A., and Paes, D. A. (2022). Plant Metabolites as SARS-CoV-2 Inhibitors Candidates : In Silico and In Vitro Studies, *Pharmaceuticals*. doi:10.3390/ph15091045.
12. Alzahrani, A. (2022). A New Investigation into the Molecular Mechanism of Andrographolide towards Reducing Cytokine Storm, *Molecules*, Vol. 27, No. 14. doi:10.3390/molecules27144555.
13. Maulydia, N. B., Khairan, K., Tallei, T. E., Estevam, E. C., Patwekar, M., Mohd Fauzi, F., and Idroes, R. (2023). GC-MS Analysis Reveals Unique Chemical Composition of Blumea balsamifera (L.) DC in Ie-Jue Geothermal Area, *Grimsa Journal of Science Engineering and Technology*, Vol. 1, No. 1, 9–16.
14. Daina, A., Michielin, O., and Zoete, V. (2017). SwissADME: A Free Web Tool to Evaluate Pharmacokinetics, Drug-Likeness and Medicinal Chemistry Friendliness of Small Molecules, *Scientific Reports*, Vol. 7, No. March, 1–13. doi:10.1038/srep42717.

15. Lipinski, C. A. (2016). Rule of Five in 2015 and Beyond: Target and Ligand Structural Limitations, Ligand Chemistry Structure and Drug Discovery Project Decisions, *Advanced Drug Delivery Reviews*, Vol. 101, 34–41. doi:10.1016/j.addr.2016.04.029.

16. Kim, S., Chen, J., Cheng, T., Gindulyte, A., He, J., He, S., Li, Q., Shoemaker, B. A., Thiessen, P. A., Yu, B., Zaslavsky, L., Zhang, J., and Bolton, E. E. (2023). PubChem 2023 update, *Nucleic Acids Research*, Vol. 51, No. D1, D1373–D1380. doi:10.1093/nar/gkac956.

17. Dallakyan, S., and Olson, A. J. (2015). Small-Molecule Library Screening by Docking with PyRx, *Methods in Molecular Biology*, Vol. 1263, No. January, 243–250. doi:10.1007/978-1-4939-2269-7_19.

18. Berman, H. M., Battistuz, T., Bhat, T. N., Bluhm, W. F., Bourne, P. E., Burkhardt, K., Feng, Z., Gilliland, G. L., Iype, L., Jain, S., Fagan, P., Marvin, J., Padilla, D., Ravichandran, V., Schneider, B., Thanki, N., Weissig, H., Westbrook, J. D., and Zardecki, C. (2002). Biological Crystallography The Protein Data Bank, *Acta Cryst*, Vol. 58, 899–907.

19. Soy, M., Keser, G., Atagündüz, P., Tabak, F., Atagündüz, I., and Kayhan, S. (2020). Cytokine Storm in COVID-19: Pathogenesis and Overview of Anti-Inflammatory Agents Used in Treatment, *Clinical Rheumatology*, Vol. 39, No. 7, 2085–2094. doi:10.1007/s10067-020-05190-5.

20. Biovia. (2020). Biovia Discovery Studio® 4.5 Comprehensive Modeling and Simulations for Life Sciences, 1–3.

21. Trott, O., and Olson, A. J. (2009). AutoDock Vina: Improving the Speed and Accuracy of Docking with a New Scoring Function, Efficient Optimization, and Multithreading, *Journal of Computational Chemistry*, Vol. 31, No. 2, NA-NA. doi:10.1002/jcc.21334.

22. Schöning-Stierand, K., Diedrich, K., Ehrt, C., Flachsenberg, F., Graef, J., Sieg, J., Penner, P., Poppinga, M., Ungethüm, A., and Rarey, M. (2022). ProteinsPlus: A Comprehensive Collection of Web-Based Molecular Modeling Tools, *Nucleic Acids Research*, Vol. 50, No. W1, W611–W615. doi:10.1093/nar/gkac305.

23. Humphrey, W., Dalke, A., and Schulten, K. (1996). VMD: Visual Molecular Dynamics, *Journal of Molecular Graphics*, Vol. 14, 33–38.

24. Phillips, J. C., Braun, R., Wang, W., Gumbart, J., Tajkhorshid, E., Villa, E., Chipot, C., Skeel, R. D., Kalé, L., and Schulten, K. (2005). Scalable Molecular Dynamics with NAMD, *Journal of Computational Chemistry*, Vol. 26, No. 16, 1781–1802. doi:10.1002/jcc.20289.

25. Jo, S., Kim, T., Iyer, V. G., and Im, W. (2008). CHARMM-GUI: A Web-Based Graphical User Interface for CHARMM, *Journal of Computational Chemistry*, Vol. 29, No. 11. doi:10.1002/jcc.

26. Lipinski, C. A., Lombardo, F., Dominy, B. W., and Feeney, P. J. (2001). Experimental and Computational Approaches to Estimate Solubility and Permeability in Drug Discovery and Development Settings, *Advanced Drug Delivery Reviews*, Vol. 46, Nos. 1–3, 3–26. doi:10.1016/S0169-409X(00)00129-0.

27. Rachmawati, R., Idroes, R., Suhartono, E., Maulydia, N. B., and Darusman, D. (2022). In Silico and In Vitro Analysis of Tacca Tubers (Tacca leontopetaloides) from Banyak Island, Aceh Singkil Regency, Indonesia, as Antihypercholesterolemia Agents, *Molecules*, Vol. 27, No. 23. doi:10.3390/molecules27238605.

28. Stanzione, F., Giangreco, I., and Cole, J. C. (2021). Use of Molecular Docking Computational Tools in Drug Discovery, *Progress in Medicinal Chemistry* (1st ed., Vol. 60), Elsevier B.V., 273–343. doi:10.1016/bs.pmch.2021.01.004.

29. Bakrim, S., Benkhaira, N., Bourais, I., Benali, T., Lee, L. H., El Omari, N., Sheikh, R. A., Goh, K. W., Ming, L. C., and Bouyahya, A. (2022, September). Health Benefits and Pharmacological Properties of Stigmasterol, *Antioxidants*, 1912. doi:10.3390/antiox11101912.

30. Kamaz, Z., Jassani, M. J. A.-, and Haruna, U. (2020). Screening of Common Herbal Medicines as Promising Direct Inhibitors of Sars-Cov-2 in Silico, *Annual Research & Review in Biology*, Vol. 35, No. 8, 53–67. doi:10.9734/arrb/2020/v35i830260.

31. El-Askary, H. I., Meselhy, M. R., and Galal, A. M. (2003). Sesquiterpenes from Cymbopogon proximus, *Molecules*, Vol. 8, No. 9, 670–677. doi:10.3390/80900670.

32. Maulydia, N. B., Khairan, K., and Noviandy, T. R. (2023). Prediction of Pharmacokinetic Parameters from Ethanolic Extract Mane Leaves (Vitex pinnata L.) in Geothermal Manifestation of Seulawah Agam Ie-Seu'um, Aceh, *Malacca Pharmaceutics*, Vol. 1, No. 1, 16–21. doi:10.60084/mp.v1i1.33.